Available online at www.sciencedirect.com
ScienceDirect
Cement and Concrete Research 37 (2007) 1022–1034
Cement and Concrete Research

A review of salt scaling: II. Mechanisms

John J. Valenza II *, George W. Scherer

Princeton University, Civil and Env. Engr./Princeton Inst. Sci. & Tech. Mat., 70 Prospect St., Rm. 218 Bowen Hall, Princeton, NJ 08540, USA

Received 8 August 2006; accepted 5 March 2007

Abstract

Salt scaling is a major durability issue for concrete. Despite this, and an extensive research effort, the cause of this damage is unknown. Therefore, no means for preventing salt scaling can be identified. One of the primary reasons for this shortcoming is the lack of a critical review on the state of the research in this field. Such a compilation is presented in this series of articles. In Part I, the characteristics of salt scaling were outlined. In this article, proposed mechanisms are discussed, and their adequacy is judged based on their ability to account for the phenomenology.

Keywords: Salt scaling; Mechanisms; Internal crystallization; Role of salts; Glue spalling

Contents

1. Introduction

Concrete is the most widely used material in the world. The raw materials are ubiquitous, so it is relatively inexpensive, but concrete poses numerous durability issues that result in high maintenance costs. The National Research Council estimates that repair of the infrastructure in the United States costs nearly $50 Billion annually [1]. Moreover, the cost of new roadways, bridges, and terminals is estimated at hundreds of billions of dollars annually. Clearly, improving the durability of concrete has huge social and economic implications.

Over the past 60 years, concrete infrastructure has deteriorated by “salt scaling”, which is superficial damage caused by freezing a saline solution on the surface of a cementitious body (Fig. 1). The damage is progressive and consists of the removal

* Corresponding author. Hampshire St., Cambridge, MA 02139, USA. Tel.: +1 6177682346; fax: +1 6177682386.
E-mail address: jvalenza@slb.com (J.J. Valenza).

0008-8846/$ - see front matter © 2007 Published by Elsevier Ltd.
doi:10.1016/j.cemconres.2007.03.003

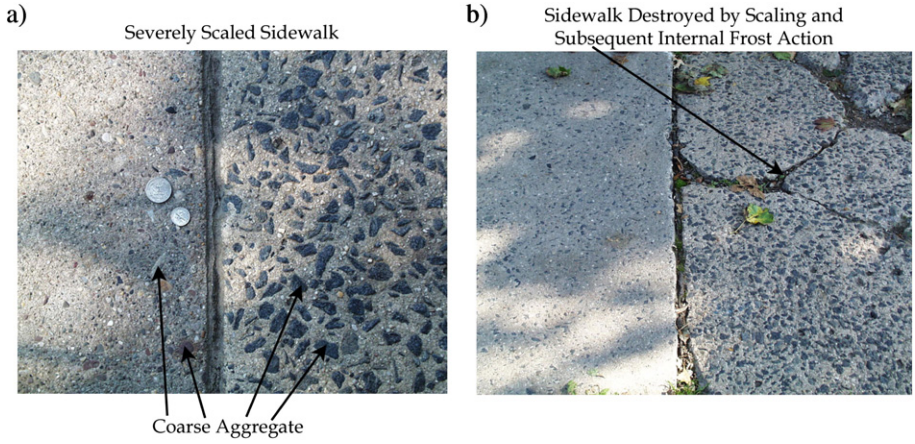

Fig. 1. (a) Picture of a severely scaled sidewalk. (b) Sidewalk that was severely scaled, which led to a complete loss of mechanical integrity, probably by internal frost damage.

of small chips or flakes of material. These characteristics were first revealed in the 1950s through laboratory testing [2,3], and they were subsequently verified through field tests [4]. In moderate to extreme cases, this damage culminates in the exposure of the coarse aggregate.

In cold climates, salts (NaCl, $CaCl_2$) are regularly used to de-ice roadways and walkways. Consequently, salt scaling is one of the major durability issues facing cementitious materials in this climate. While salt scaling alone will not render a structure useless, it results in accelerated ingress of aggressive species, such as chlorides, and the propensity for a high degree of saturation. The former renders the body susceptible to corrosion of the reinforcing steel [5–7], while the latter results in strength loss from internal frost action [8–10]. Both of these effects diminish the service life of concrete (Fig. 1).

Hundreds of laboratory and field studies have clearly identified the characteristics of salt scaling, but have not explained the cause. In a companion article [11] this work was critically reviewed, and the following list of characteristics was compiled:

1. Salt scaling consists of the progressive removal of small flakes or chips of binder.
2. A pessimum exists at a solute concentration of ~3%, independent of the solute used.
3. No scaling occurs when the pool of solution is missing from the concrete surface.
4. No damage occurs when the minimum temperature is held above −10 °C; the amount of damage increases as the minimum temperature decreases below −10 °C and with longer time at the minimum temperature.
5. Air entrainment improves salt scaling resistance.
6. The salt concentration of the pool on the surface is more important than the salt concentration in the pore solution.
7. Susceptibility to salt scaling is not correlated with susceptibility to internal frost action.
8. The strength of the surface governs the ability of a cementitious body to resist salt scaling.

A number of mechanisms for salt scaling have been proposed. In the next two sections, we consider the ability of these mechanisms to account for the above characteristics. First, in Section 2 we consider mechanisms related to internal crystallization. Then in Section 3 we consider mechanisms related to the role of salt. In Section 4, we consider a new, purely physical mechanism known as glue spalling. Finally, we summarize the implications of our analysis in Section 5.

2. Internal crystallization

In spite of evidence that indicates the distinct nature of salt scaling and internal frost action [11], considerable attention has been paid to internal crystallization as a cause of salt scaling. Therefore, in the interest of completeness it is necessary to discuss this topic. Much of the discussion follows analyses by Scherer [9] and Scherer and Valenza [10] that consider the thermodynamics of crystallization in a porous medium. The role of hydraulic pressure is considered in Section 2.1 and crystallization pressure in Section 2.2.

2.1. Hydraulic pressure

The specific volume of ice is 9% greater than the water from which it forms. When ice forms in a porous medium this volume increase results in a flux away from the zone of freezing. Powers [12] suggested that the hydraulic pressure that drives this flux is the cause of damage from internal frost action. In a porous medium this flux obeys Darcy's Law:

$$J = -\frac{k}{\eta_L}\nabla p = -\frac{k}{\eta_L}\left(\frac{P_L - P_e}{L}\right) \quad (1)$$

where, J (m/s), is the fluid flux, k (m^2), is the permeability, η_L (Pa s) is the fluid viscosity, P_L is the pressure in the pore fluid, P_e is the ambient pressure, and L is the distance over which the pressure gradient in the pore fluid, ∇p, exists. To limit the pressure that arises upon freezing, Powers suggested reducing the average distance between air voids in concrete [13,14] (i.e., air voids represent escape boundaries where the pressure is P_e). In a later study, Powers and Helmuth [15] verified that limiting the average air void spacing to

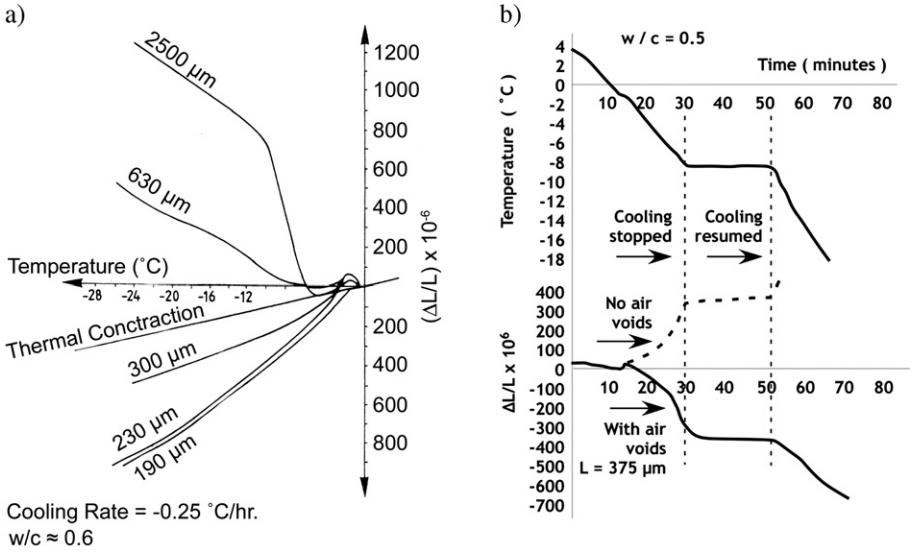

Fig. 2. Results from reference [15]. (a) Volume change is reversed by reducing the average air void spacing. (b) Dilation of a non-air-entrained sample does not relax during the isotherm, and contraction of an air-entrained sample does not immediately stop when cooling is arrested.

250–300 μm (Fig. 2a) prevents deleterious expansion upon internal crystallization.

The results from reference [15] show that as the air void spacing is reduced the volume change is reversed (Fig. 2a). When cooling is arrested, dilation of a non-air-entrained sample does not relax away (Fig. 2b, dashed curve) [15]. Hydraulic pressure does not account for either of these observations. The adequately air-entrained paste contracts upon freezing, because ice crystals on the surface of the air voids suck water from the surrounding porous matrix (Fig. 3) [10]. It is a common misconception that this contraction is a result of ice melting in the capillary pores and the diffusion of gel water to ice in the air voids [15]. In the next section it will be shown that ice in the capillary pores is in equilibrium with ice in air voids. Osmotic pressure is also excluded, as it can be shown (see Section 3.3.2) that hydrodynamic relaxation quickly dissipates the pressure gradient caused by diffusion.

When ice forms on the external surface of a porous medium, the crystals bulge into the mouths of surface pores (Fig. 3). The curvature of the crystal/liquid interface, κ_{CL}, in a pore is given by [10]:

$$P_A + \gamma_{\mathrm{CL}}\kappa_{\mathrm{CL}} = -\Delta V_{\mathrm{CL}}\gamma_{\mathrm{LV}}\kappa_{\mathrm{LV}} + \Delta S_{fC}(T_m - T) \tag{2}$$

where P_A is pressure applied to the crystal only, γ is the interfacial energy, κ is the curvature, $\Delta S_{fC}=(S_L-S_C)/v_C$ is the entropy of fusion per unit volume of ice, $\Delta V_{\mathrm{CL}}=(v_C-v_L)/v_C$ is the fractional volume change that accompanies solidification, $\Delta T=T_m-T$, is the undercooling, T_m is the melting point of the solution (in this case bulk water), S is the entropy, v is the molar volume, the subscripts CL and LV indicate quantities that correspond to the crystal/liquid and liquid/vapor interfaces respectively, and the subscripts C and L indicate quantities that correspond to the crystal and liquid respectively. The pressure in the liquid, P_L, adjacent to the bulging crystal is [10]:

$$(P_L - P_{\mathrm{E}}) = -\Delta S_{fL}(T_m - T) = \gamma_{\mathrm{LV}}\kappa_{\mathrm{LV}} \tag{3}$$

where P_{E} is the equilibrium vapor pressure of bulk ice (Fig. 3), and the second equality follows from Laplace's equation [16]

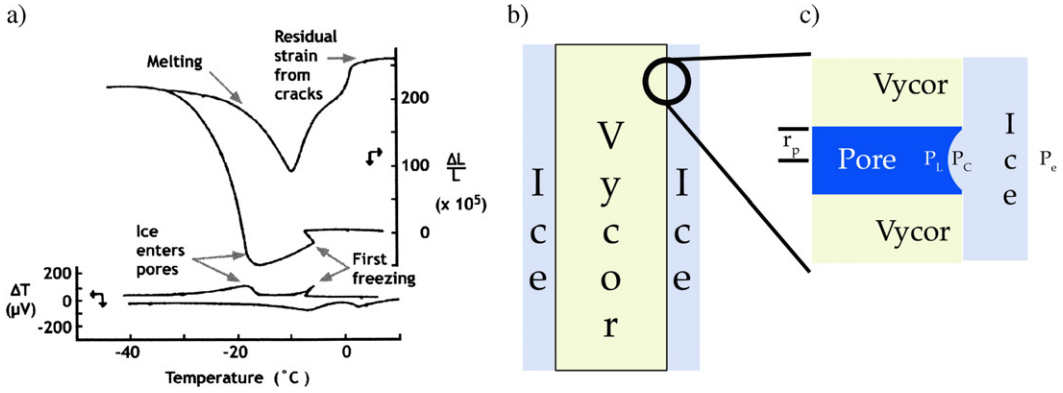

Fig. 3. (a) Dilation of a saturated Vycor® plate that is frozen [18]. The plate contracts until the temperature reaches, $T=-17$ °C. (b) Schematic of ice forming on the external surface of a Vycor® plate, indicative of the experiments discussed in reference 18. (c) Schematic of ice on the surface of the Vycor®, bulging into the mouth of a surface pore.

(note: here $\Delta S_{fL}=(S_L-S_C)/v_L$). When ice bulges into the pore mouth there is no restraint on the crystal/liquid interface ($P_A=0$), and $\Delta S_{fL}=1.3$ J/cm^3 K [17], so $P_L=P_E-1.3\Delta T$ (the parameter P_E is included for rigor. However, under normal ambient conditions this pressure is 3 to 4 orders of magnitude smaller than P_L, so it can be set to zero, $P_E=0$, with the introduction of very little error). It is this suction that causes air-entrained samples to contract.

Litvan observed this relationship between pore pressure, P_L, and undercooling, ΔT, when measuring the dilation of saturated Vycor® upon freezing [18]. He observed that ice first formed on the surface of the Vycor® (Fig. 3). The ice on the surface imposed the freezing suction in the pore fluid, which forced the body to contract (Fig. 3). The thermal contraction strain was on the order of 3.3×10^{-5}/°C. The mechanical response of a saturated porous body with pressure in the pore fluid was determined by Biot and Willis [19–22] and expressed in terms of conventional parameters by Johnson [23], Coussy [24], and Scherer [25]:

$$\varepsilon_x = \frac{P_L}{3K_P}\left(1-\frac{K_P}{K_S}\right) \tag{4}$$

where K is the bulk modulus, and the subscripts P and S indicate values that correspond to the drained porous network and the solid phase, respectively. The bulk modulus of Vycor® is $K_P\approx7.8$ GPa, and the modulus ratio is estimated to be $K_P/K_S\approx0.42$ [26]. Therefore, Eq. (4) indicates that the pressure driving contraction of the Vycor® is $P_L=-(3.3\times10^{-5})(3)(7.8\times10^9)/0.58=-1.3$ MPa/°C, which agrees with the theoretical prediction.

The curvature of a spherical air void in cement paste ($r_p=50$–500 μm) is 4–5 orders of magnitude larger then that of the "gel" pores in the paste ($r_p=2$–50 nm), so the surface of an air void is approximated as an external surface. When ice forms on the surface of an air void [27], it imposes the pore pressure (suction) in the pore fluid on the surrounding porous matrix. The analysis we applied to Litvan's results can be used to interpret the experiments by Powers et al. (Fig. 2b). In our laboratory we found the elastic modulus of cement paste with $w/c=0.6$ to be $E_P=12$ GPa [28]; assuming Poisson's ratio to be $v=0.2$, the bulk modulus is $K_P=E_P/3(1-2v)=6.7$ GPa. Reference [28] indicates that the modulus ratio obeys the power law, $K_P/K_S=\rho^2$, where $\rho=0.5$ is the volume fraction of solids [28]. The thermal expansion coefficient of cement paste is 10^{-5}/°C [29], so the strain exerted by the pore pressure is 2.5×10^{-5}/°C, and the magnitude of the pore pressure is $P_L=-(2.5\times10^{-5})(3)(6.7\times10^9)/0.75=-0.7$ MPa/°C. The discrepancy between this value and the theoretical value (45%) is attibuted to crystallization pressure in the capillary pores, which is discussed in the next section.

Fagerlund demonstrated that deterioration of concrete by internal frost action occurs rapidly once a critical degree of saturation is achieved [30]. He suggests that the main cause of damage is hydraulic pressure that is exacerbated by the reduction in permeability caused by internal ice formation. The critical degree of saturation is observed to be between 80 and 90% [30] and necessitates 100–200 days of continuous immersion [31–33]. Such conditions are not met during a salt scaling test, which lasts no more than 60 days, and it is not likely that they are met in practice. This high degree of saturation renders a considerable fraction (~50%) of the air voids saturated [30,33].

For two hypothetical, but realistic, air void systems, Fagerlund estimated the size of the largest filled void at the critical degree of saturation to be ~100 μm [33]. The growth rate of ice, U, measured in a glass capillary tube [34] is:

$$U = 1.6\Delta T^{1.7}\text{mm/s} \tag{5}$$

Therefore, at an undercooling of only $\Delta T=3$ °C, the growth rate is 1.3 cm/s and a saturated air void ($r_p=100$ μm) will crystallize in less than 1/1000 s. The velocity of the water forced out of the air void is $U/(1-\rho)\approx1.3/0.5=2.6$ cm/s. Assuming the void spacing at this saturation is $L\sim400$ μm [33], the viscosity of water at −3 °C, $\eta_L=0.003$ Pa s, and the permeability, $k=10^{-19}$ m^2, then from Eq. (1) the estimated hydraulic pressure from freezing in the air voids is $P_L\approx(0.026)(0.003)(4\times10^{-4})/10^{-19}\approx312$ GPa (ambient pressure, P_e, is set to zero). Of course such high pressures are not possible, because the ice would be forced to melt. The fluid pressure is limited by the Clausius-Clapeyron condition [35]:

$$\left(\frac{dP_L}{dT}\right)_{\Delta G=0} = \frac{\Delta S_{fL}}{\Delta V_{CL}} = 13.5\ \text{MPa/°C} \tag{6}$$

Eq. (6) indicates the pressure from crystallization in saturated air voids will exceed the tensile strength (~3 MPa) of cement at small undercoolings, $\Delta T\approx0.25$ °C. Heterogeneous nucleation in bulk water is routinely observed at much greater (5–15 °C) undercoolings; therefore it is likely that damage of saturated concrete is a result of bursting of water-filled air voids, owing to the expansion of the ice. Note that this is not equivalent to the usual mechanism of hydraulic pressure.

2.2. Crystallization pressure

The results presented in Fig. 2 led Powers to retract the hydraulic pressure hypothesis [36]. Helmuth shared this sentiment, and later suggested that crystallization pressure was the main cause of frost damage [37]. The predominance of crystallization pressure is demonstrated by the fact that porous bodies are damaged when they are frozen containing liquids that do not have a smaller specific volume than the corresponding solid [38,39]. The mechanisms by which this damage occurs are discussed below.

When solidification occurs in a fine pore ($r_p<50$ nm) the melting point is reduced, because the crystals have a high surface to volume ratio. The energy of the system is not minimized by solidification at the melting point of bulk water, because the energy gained by solidification of a small volume is offset by the energy of the crystal/liquid interface. The Gibbs-

Thomson equation provides the relationship between the melting point and the curvature of a small crystal [9]:

$$T = T_m - \frac{\gamma_{CL}\kappa_{CL}}{\Delta S_{fC}} \tag{7}$$

Therefore, the relationship between the melting point, T, and the largest spherical crystal that can fit in a pore with radius, r_p, is:

$$T = T_m - \frac{2\gamma_{CL}}{(r_p - \delta_w)\Delta S_{fC}} \tag{8}$$

where $\delta_W \approx 0.9$ nm is the thickness of the unfrozen water layer between the crystal and the pore wall [17]. Eq. (8) indicates that the melting point is reduced by 2 °C for $r_p \approx 33$ nm, by 5 °C for $r_p \approx 13$ nm, and by 10 °C for $r_p \approx 7$ nm.

Eq. (8) provides the relationship between the temperature and the size of the pore that ice can penetrate from a larger pore, void (Fig. 5), or external surface (Fig. 3). This is illustrated in the results reported by Litvan [18], presented in Fig. 3. Initially ice forms on the exterior of the Vycor® plate and the sample contracts until a temperature of $T = -17$ °C. At this temperature, there is a hump in the thermogram (bottom of Fig. 3a), which corresponds to internal crystallization (penetration of the external ice). At $T = -17$ °C, Eq. (8) indicates that ice is capable of entering pores with a radius of $r_p \approx 4$ nm, which is reasonable for Vycor®. This material has a very narrow pore size distribution, so once the ice penetrates the interior it is capable of accessing a majority of the microstructure. As the ice invades the microstructure the plate begins to dilate.

Consider a hypothetical cylindrical crystal in a pore of radius, r_p (Fig. 4). Here the hemispherical end (E) of the crystal and the cylindrical body (B) adopt the radius $r_p - \delta_W$. The pressure in the liquid, P_L, and the temperature are such that Eq. (2) is satisfied with $P_A = 0$ and κ_{CL} corresponding to the hemispherical end (E). As a result of the difference in curvature between the side [$\kappa_{CL} = 1/(r_p - \delta_W)$] and the end [$\kappa_{CL} = 2/(r_p - \delta_W)$] of the crystal, the crystal attempts to grow in the direction of the pore wall. To suppress this growth and satisfy mechanical equilibrium in the crystal, the wall must apply a radial compressive pressure on the cylindrical body of the crystal:

$$P_A = \gamma_{CL}\left(\kappa_{CL}^{E} - \kappa_{CL}^{B}\right) = \frac{\gamma_{CL}}{\left(r_P^B - \delta_W\right)} \tag{9}$$

The repulsion between the crystal and the pore wall is so large that the pressure necessary to force them into contact is greater than the tensile strength of cement paste or Vycor® glass [9]. Therefore, the film of fluid persists and the crystal attempts to grow towards the wall, pushing the wall away [40–42]. This is the same mechanism that causes frost heave [43–47]. This crystallization pressure, P_A, causes a tensile hoop stress in the pore wall, $\sigma_\theta \approx P_A/2$. Assuming that the tensile strength of the cementitious binder is 3 MPa, this implies that the binder will be damaged when ice forms in cylindrical pores with $r_p < 7.6$ nm, which corresponds to a melting point of $T = -10$ °C according to Eq. (8).

The pore geometry in Fig. 4 is overly simplified: binder in concrete has pores with irregular shapes, consisting of cavities with constrictions at the points of entry (i.e., $r_P^B > r_P^E$), otherwise known as inkbottle pores [48]. In addition, the pore and void sizes range over 5–6 orders of magnitude [49,50]. Consider the more realistic situation illustrated in Fig. 5, where the temperature is such that ice has formed in the air void (on the right) and in the larger cavity of the capillary. At this temperature, the ice is unable to obtain the curvature necessary to penetrate the conduits between the capillary cavity and the air voids. At equilibrium, the pressure in the pore fluid is determined by the curvature of the crystal bulging into the mouth of the conduit from the air void (N), which is identical to the curvature of the crystal at E. In the previous section it was shown that the freezing suction, imposed by the crystal/liquid interface at (N), is $P_L = -\gamma_{CL}\kappa_{CL}^{N} \approx -1.3\Delta T$. To support this suction, the liquid/vapor (LV) meniscus forms at (A) (on the left) with curvature found from Eqs. (2) and (3) [35,51]:

$$\kappa_{LV} = -\frac{\gamma_{CL}\kappa_{CL}}{\gamma_{LV}} \tag{10}$$

Stress arises in the pore wall as the crystal attempts to grow. Eq. (9) indicates that when the curvature of the ice body is positive the pressure necessary to prevent growth, P_A, is less than the suction imposed on the pore fluid, P_L (viz., $P_A \approx P_L/2$). Therefore, once the fluid pressure equilibrates with the suction imposed at N and E in Fig. 5, the net hoop stress in the capillary cavity will be compressive. This statement is true, whether or not ice forms in the air void, because liquid/vapor menisci (A in Fig. 5) will support the suction imposed by the crystal/liquid interface at E. At point F in Fig. 5, the curvature of the ice body is negative, so the pressure necessary to prevent growth is greater than the suction in the pore fluid: $P_A = \gamma_{CL}(\kappa_{CL}^{E} - \kappa_{CL}^{F}) = -P_L - \gamma_{CL}\kappa_{CL}^{F}$. Therefore, the ice in the cavity creates hoop tension in the wall at (F) after the pore fluid equilibrates at P_L.

This analysis indicates that ice can exist in the capillaries and in the air voids simultaneously, because of the suction in the

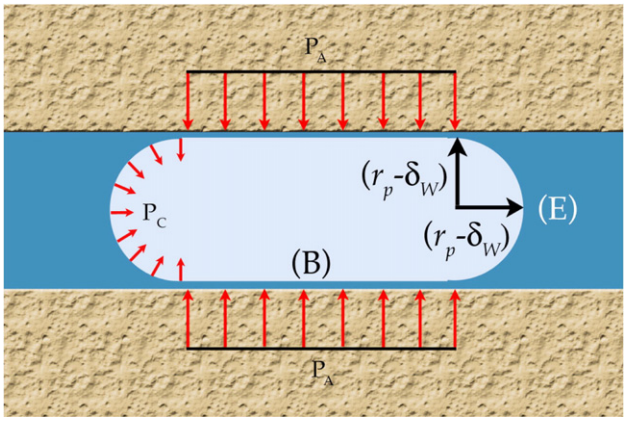

Fig. 4. Schematic of a cylindrical crystal in a pore of radius r_p. Both the hemispherical end (E) and the cylindrical body (B) adopt the radius, $r_p - \delta_W$.

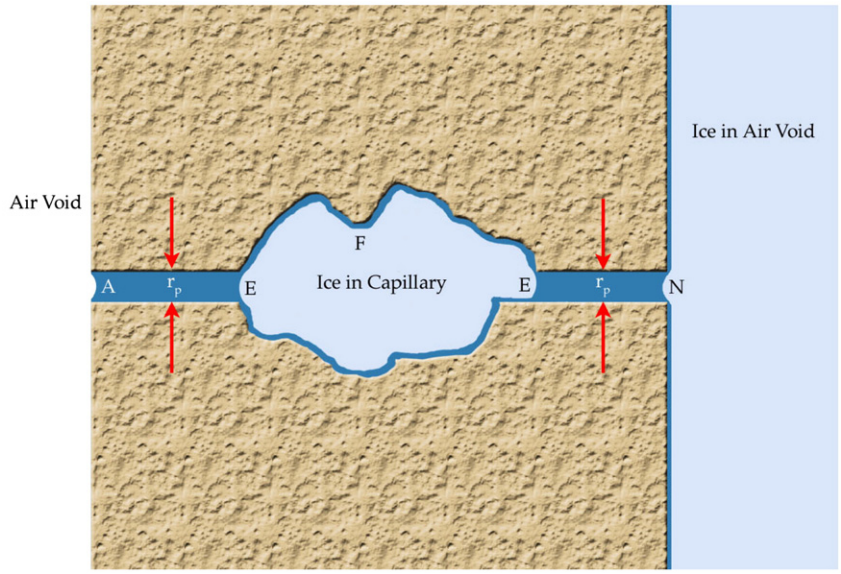

Fig. 5. Schematic of ice forming in a capillary cavity and in an air void. The temperature is such that the ice cannot obtain the curvature (Eq. (7)) necessary to penetrate the conduits between the cavity and the air voids.

pore fluid. At equilibrium, crystals in the capillary can exert pressure on the wall at points where the curvature of the crystal is negative (*F*). It is the pressure at these points that contributes to the discrepancy between the theoretical pore pressure and that calculated from the results of Powers et al. (Fig. 2). In addition, when the ice penetrates the pores (i.e., when the curvature at *E* or *N* reaches $2/(r_p-\delta)$, but before the liquid pressure equilibrates), it imposes crystallization pressure on the pore walls. It is this crystallization pressure that causes the initial dilation illustrated in Fig. 2 at $T=-2$ °C. The air-entrained paste eventually contracts as ice in the air voids imposes suction on the pore fluid. The time over which this dilation relaxes away is governed by the transport properties of the body, and is therefore characteristic of the material. Overall, the air-entrained paste exhibits contraction (Fig. 2) because once equilibrium is established the majority of the internal surface is exposed to the (negative) pore pressure, P_L.

This analysis [10,52] also accounts for the transient contraction observed when cooling is arrested (Fig. 2b — air-entrained paste). The sample continues to contract, because the pressure in the pore fluid is equilibrating with the pore pressure at the crystal/liquid interface (*N* — Fig. 5). As the temperature is reduced, the pore pressure at the interface (*N*) becomes more negative because the interfacial curvature increases. Therefore, there is a difference between suction at the interface and greater fluid pressure elsewhere. During an isotherm, fluid flow alleviates this gradient according to Eq. (1) and the curved liquid/vapor meniscus will form (*A*) or the suction will be supported by an equivalent liquid/crystal interface at the mouth of a connecting pore (*N*).

Fig. 2 indicates that the transient expansion (Fig. 2a, $T=-2$ °C) and contraction (Fig. 2b, $T=-8$ °C) relax in a period of roughly 7 min. For similar, intentionally saturated material, at 29 °C we measured a hydrodynamic relaxation time, $\tau_R \approx 700$ s [53]. The relaxation time is proportional to the viscosity and the distance over which flow occurs ($\tau_R \propto \eta_L L^2$); taking into account the three-fold increase in η_L between the temperature of our experiment and that of Powers, we estimate that the average distance over which relaxation occurs is $L \approx 450$ μm. The samples used by Powers et al. were cured with the intent of maintaining the highest degree of saturation possible, and the age at testing is between 3 weeks and 3 months, with some samples tested at an age of 2 years [15]. Fagerlund indicates that after complete submersion for 3 months to 1 year (depending on the shape of the air-void size distribution) the spacing factor increases to $L \approx 400$ μm from the filling of voids [33]. Therefore, it is plausible that the transient volume changes illustrated in Fig. 2 are a result of hydrodynamic relaxation.

The freezing suction, P_L, arises at the crystal/liquid interface (*N*) and propagates through the pore network as hydrodynamic relaxation occurs. Thus, at the instant that growth begins, crystals in capillary cavities will impose crystallization pressure, P_A, at all points adjacent to the pore wall. This pressure is eventually offset as the pressure in the pore fluid is reduced, compressing the porous network. It was observed that the fluid pressure equilibrates over a period of 7 min, so there is a substantial transient during which crystallization pressure creates tensile stress in the porous skeleton.

The propensity for damage from crystallization pressure depends on: the temperature of the system, the extent of ice formation, the morphology of the capillary pores, and where initial freezing occurs. In particular, our analysis indicates that promoting initial nucleation at a small undercooling in the air voids is beneficial, and lining the voids with dense paste (i.e., reducing the pore size at *N* in Fig. 5) will prevent penetration into the capillary network until very low temperatures. To accomplish the former it has been proposed to introduce nucleating agents into the air voids [53]. For water the energy of the liquid/vapor interface is larger than that of the crystal/liquid interface; therefore, if ice forms in the air voids first, the ice will

drain the intersecting pores until the liquid/vapor meniscus enters a constriction with a size such that Eq. (10) is satisfied (A in Fig. 5). Once this condition is met, the crystal/liquid interface can no longer drain fluid from the pore because Eq. (10) requires that the crystal will penetrate the pore before the liquid/vapor meniscus passes the constriction.

Chatterji [54] reports that certain air-entraining agents (AEA) are more effective than others. It has not been determined whether this trend is a result of the ability of the AEA to nucleate ice or the affinity of the surfactants for cement particles, resulting in smaller pores in the paste surrounding the voids. However, Mielienz et al. [55] demonstrated that the most effective AEA have a higher affinity for cement grains. Therefore, it appears to be beneficial to form a dense shell of paste around the void. If ice forms in the voids first, drains some of the fluid from the intersecting capillary pores, and imposes suction in the saturated porosity, the potential for damage from crystallization pressure is greatly reduced.

As the temperature is further reduced, ice is able to access more of the porosity. When this occurs, there are two situations that can lead to the formation of damaging stress: (1) ice escapes from a large cavity or void by passing a constriction; (2) ice grows into a zone of saturated microstructure encapsulated by the invading ice. The stress that arises during the former depends on the morphology of the microstructure. The corresponding variations are analyzed elsewhere [56]. The latter situation is analogous to freezing a water drop, where a crust of ice forms on the droplet surface and the ice propagates toward the interior. In this case the pressure in the confined water rises quickly but is limited by Eq. (6). Even with this limitation, at $T=-1$ °C the fluid pressure is 13.5 MPa, and the corresponding stress in the pore wall is well above the tensile strength of concrete. Fagerlund [56] and Chatterji [54] previously suggested that damage is caused when pockets of water are surrounded by ice and the fluid pressure increases as the ice invades the trapped pores.

2.3. Summary

Experimental results indicate that hydraulic pressure is not responsible for the damage from internal crystallization. Analysis of the thermodynamics of internal crystallization and allowing for hydrodynamic relaxation accounts for all characteristics of the experimental results (Figs. 2 and 3) obtained with properly air-entrained cement paste or Vycor® glass. Adequately air-entrained concrete will be immune to internal frost action, if initial ice formation occurs in the air voids and compresses the surrounding matrix. Absence of adequate air entrainment results in destructive dilation from crystallization pressure. The critical air void spacing indicates the average distance at which the majority of the body will be compressed upon internal freezing. If the surface of the body is adequately air-entrained, the suction imposed by ice in these air voids might also aid in preventing salt scaling. Once the temperature is low enough to allow the ice to propagate through a majority of the microstructure, destructive stresses are expected.

To evaluate the importance of crystallization pressure as the cause of salt scaling, it is necessary to consider the effect salt has on these mechanisms. It is shown below that after very short times (2–5 days, Fig. 7) the salt concentration in the surface will equilibrate with the concentration of the outer solution. Since the amount of ice that forms decreases with increasing salt concentration [57–59], it is expected that pure water would yield the most salt scaling if either hydraulic pressure or crystallization pressure was responsible for salt scaling. Therefore, neither of these mechanisms can account for the pessimum concentration. In addition, these mechanisms do not account for the lack of damage when the pool of solution is missing from the concrete surface. For example, experiments have been performed where the sample is frozen without the solution, then thawed with the solution on the surface. This technique was determined to be less detrimental than freezing the saline solution on the surface [3].

3. Role of salt

In this section we will consider several proposed mechanisms that concern the role salt plays in salt scaling. In Section 3.1 we will consider the fact that salt reduces the melting point of ice, and how this may result in stress from thermal shock. In Section 3.2 we examine the possibility that damage is caused by the precipitation of salt in the pore system. Section 3.3.1 deals with the effect of salt on the vapor pressure of water and the corresponding degree of saturation of the cementitious surface. Finally, the role of osmotic pressure is considered in Section 3.3.2.

3.1. Thermal shock

In the presence of a salt solution, the melting point, T_m, of ice is reduced [60] (Fig. 6 — Liquidus). Accordingly, application of salt to an ice layer causes the ice to melt if the salt concentration lowers the melting point below ambient temperature. The heat necessary to cause this melting is withdrawn from the surface of the concrete body. As a result, a temperature gradient will form in the surface, resulting in differential strain and stress [61].

An approximate upper bound on the stress can be obtained by assuming that the pressure in the pore fluid is negligible and that the temperature change is limited to a small thickness near the surface. In this case, the body does not deform as a result of the stress, σ_x, in the thin layer, and there is tensile stress in the surface [62]:

$$\sigma_x = \left(\frac{E_p}{1-\nu}\right)\alpha\Delta T \tag{11}$$

Reference [61] indicates that ~80% of the time when salt is applied to ice on the surface of a concrete body, the temperature of the surface is reduced by ~1 °C. For a concrete sidewalk with, $E_P \approx 30$ GPa, $\alpha = 10^{-5}$/°C, and $\nu = 0.2$, Eq. (11) indicates that the maximum stress in the surface from a temperature change of $\Delta T = -1$ °C is, $\sigma_x \approx 0.34$ MPa. In order to approach the tensile strength of the concrete (~3 MPa), Eq. (11) indicates that the necessary temperature drop at the surface is $\Delta T = 8$ °C.

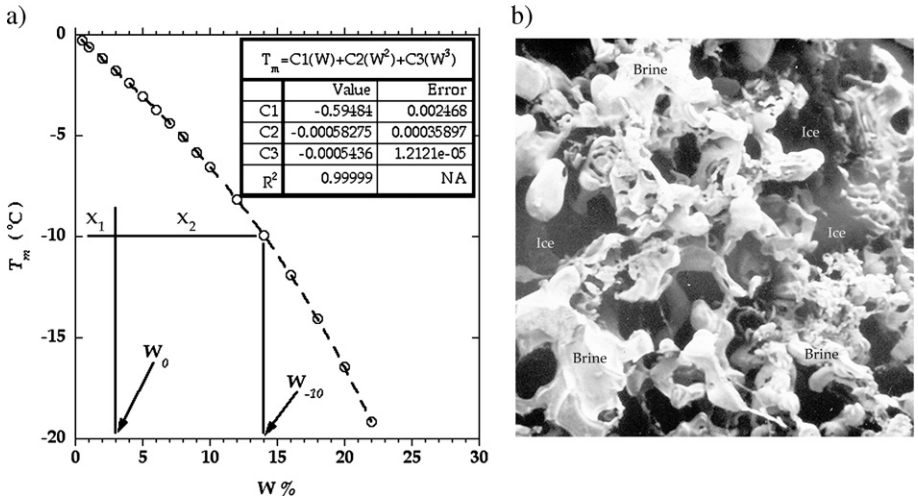

Fig. 6. (a) NaCl-H_2O liquidus; illustrating the lever rule (i.e. at −10 °C the volume fraction of ice is determined by, $\varphi = 1 - x_1/x_2 = 1 - W_0/W_{-10}$). (b) Picture of epoxy impregnated brine ice, where the epoxy fills the brine pockets [63].

Reference [61] indicates that such a drastic shock never occurs in the field. In addition, this mechanism does not account for the pessimum concentration, and it does not apply to most laboratory experiments, which involve freezing a saline solution on the surface of a concrete body, rather than applying salt on top of existing ice. In fact, it was empirically verified that freezing a saline solution on the surface is more destructive than applying salt to ice on the surface of a concrete slab [3]. Therefore, we conclude that thermal shock is not a significant contributor to salt scaling damage.

3.2. Precipitation and growth of salt

When a saline solution is frozen, the ice does not incorporate any of the dissociated salt ions in the crystal lattice [63] (Fig. 6b). Therefore, the concentration of salt in the remaining solution increases. The concentration of the solution in equilibrium with ice at any temperature below the melting point can be determined from the corresponding point on the liquidus curve in the phase diagram (Fig. 6 — $NaCl/H_2O$ system). This means that the surface of a sample in a salt scaling experiment is exposed to a concentrated solution whose composition depends on the minimum temperature imposed. At any temperature, the equilibrium volume fractions of ice and brine can be determined by the lever rule [64] with the knowledge of the initial solution concentration. The volume of the concentrated solution decreases as the initial solution concentration decreases. For a 3 wt.% solution of NaCl at −20 °C the concentration of the remaining solution in contact with the sample is ~22 wt.% NaCl, and the volume fraction of solution is ~5%.

Precipitation of salt has been suggested as a possible cause of salt scaling [65,66]. To test the viability of this mechanism, we will consider the specific case of sodium chloride (NaCl), one of the most common deicers. At room temperature a NaCl solution is saturated at ~26 wt.% NaCl [67]. The maximum initial solution concentration used in salt scaling experiments is ~10 wt.%. Therefore, during a salt scaling experiment, precipitation of NaCl will not occur before the eutectic temperature is reached, $T = -21.1$ °C. This temperature is below the minimum temperature used in salt scaling experiments. Therefore, there is not enough salt present, nor is the minimum temperature low enough, to permit damage from salt precipitation in laboratory experiments. Furthermore, this mechanism would not account for the occurrence of the pessimum or the similar behavior of chemically dissimilar (organic and inorganic) solutes.

In practice the concentration of salt in the concrete surface will equilibrate with that of the external solution. Upon drying, the concentration of salt in the pore solution will increase and precipitation of salt will occur. It has been shown that these conditions may result in destructive stresses [68,69]. The extent of damage depends on the rate of salt application, and the rate at which salt is removed from the surface by drainage. Drying does not occur in laboratory tests for salt scaling, but it does occur in the field, so salt crystallization during drying might contribute to surface damage in practice.

3.3. Salt concentration in the pore solution

The depth at which the salt concentration in the pore fluid will equilibrate with that in the pool on the surface is estimated from $x^2 = Dt$, where x is the equilibrated depth, D is the diffusion coefficient, and t is time. At room temperature the diffusion coefficient of the chloride ion in cement-based materials is known to be 10^{-11} to 10^{-10} m^2/s [70]. Assuming that the diffusion coefficient of the sodium ion is similar, Fig. 7 shows the equilibrated depth as a function of time. Increasing the salt concentration in the pore fluid increases the degree of saturation of the surface, and reduces the amount of ice formed in the pores [57–59]. When ice forms in this environment, the salt concentration in the brine adjacent to the ice will be higher, resulting in an osmotic pressure gradient. In Section 3.3.1 we will consider how salt increases the degree of saturation in the surface and what effect this has on scaling. The effect of osmotic pressure will be considered in Section 3.3.2.

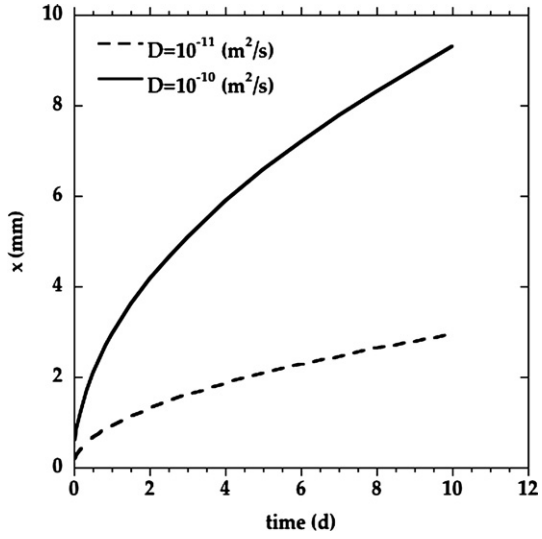

Fig. 7. Depth, x, over which the salt concentration in the pore solution will equilibrate with that of the pool on the surface. After the first few days of testing it is expected that the pore solution in the first 2–5 mm of the surface will have the same concentration as the pool.

3.3.1. Reduction in vapor pressure

Raoult's Law indicates that the vapor pressure of a dilute salt solution is lower than that of pure water [71].

$$v_s = v_b x \tag{12}$$

where, v is the vapor pressure, x is the mole fraction of water, and the subscripts, s and b, indicate values that correspond to the salt solution and bulk water, respectively. Therefore, salt dissolved in the pore solution increases the degree of saturation of concrete above that of salt free concrete, at a given relative humidity. It was previously argued by Fagerlund that internal frost action becomes detrimental at a critical degree of saturation [30]. This correlation led to the suggestion that salt scaling is the result of an increase in the degree of saturation of the concrete surface due to the presence of salt, leading to damage by internal crystallization [72,73].

It was shown above that internal crystallization does not account for the characteristics of salt scaling, most importantly the pessimum concentration. Indeed, the effect of salt on the vapor pressure is monotonic, so if this were responsible for scaling, it would get worse as the salt content increased. Moreover, moderate salt concentrations (~3%) are known to result in a drastic increase in scaling damage. However, these same concentrations will not result in a large increase in the degree of saturation [58].

3.3.2. Osmotic pressure

In Section 3.2 it was shown that the concentration of the remaining solution increases when ice forms from a salt solution. Therefore, when ice forms in the concrete surface there will be a difference in salt concentration between the zone where ice has formed and the surrounding saturated porosity. In response, there will be a tendency for water to diffuse from the zone of low concentration, to the zone of high concentration. As water diffuses towards the higher salt concentration, the fluid pressure will rise in this zone. Eventually, this pressure will be equivalent to the difference in the osmotic pressure corresponding to the two concentrations, $\Delta\Pi$, which is the pressure that must be applied to the zone of higher concentration to prevent diffusion [60]. The osmotic pressure is dictated by the difference in mole fraction of solute at the crystal/liquid interface, x, and that far from the interface, x_∞:

$$\Delta\Pi = \Pi(x) - \Pi(x_\infty) = \frac{RT}{\bar{V}_L}\ln\left(\frac{x}{x_\infty}\right) \tag{13}$$

where, R=8.314 J/mol K is the ideal gas constant, and $\bar{V}_L$ is the partial molar volume of water. Fig. 8 shows the osmotic pressure of solutions containing various amounts of NaCl. As a result of the osmotic pressure, a tensile hoop stress will arise in the pore wall, where: $\sigma_\theta \approx \Delta\Pi/2$. The potential for this stress to rise above the tensile strength occurs when the salt concentration differs by ~14%.

The osmotic pressure will never evolve to a destructive level. As the water molecules diffuse towards the zone of high concentration, causing the fluid pressure to increase there, a counteracting fluid flow described by Eq. (1) will occur. The characteristic time for the hydrodynamic relaxation of a pressure gradient, τ_R, is proportional to the square of the distance over which the gradient exists: $\tau_R \propto L^2$. In our experience, $\tau_R \approx 700$ s at 29 °C for a plate of cement paste (w/c=0.45) with L=1.5 mm [74]. Assuming that the concentration gradient occurs over a distance of 400 μm, the pressure will be relieved by fluid flow in 124 s ($\tau_R \propto L^2$). In the same paste the diffusion coefficient is estimated to be, $D \approx 1.4\times10^{-7}$ cm^2/s [75], so the concentration gradient will be alleviated by diffusion after $t = x^2/D = (0.04\ \text{cm})^2/(1.4\times10^{-7}) \approx 11.7$ h. Therefore, fluid flow prevents the formation of destructive osmotic pressure,

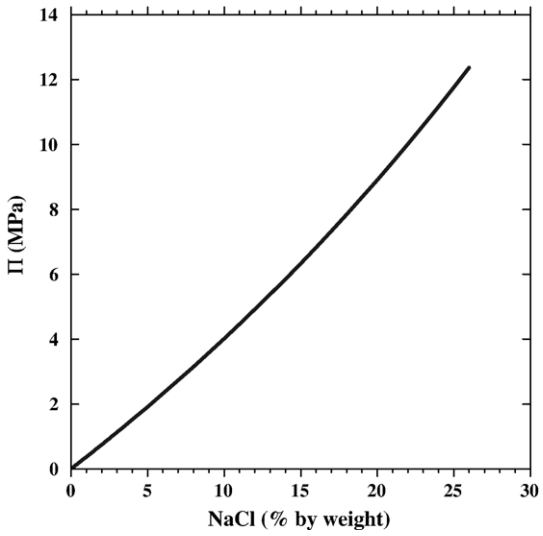

Fig. 8. Osmotic pressure calculated using Eq. (13). The stress in a pore wall from this pressure will exceed the tensile strength of cement when the concentration of salt varies by ~14%.

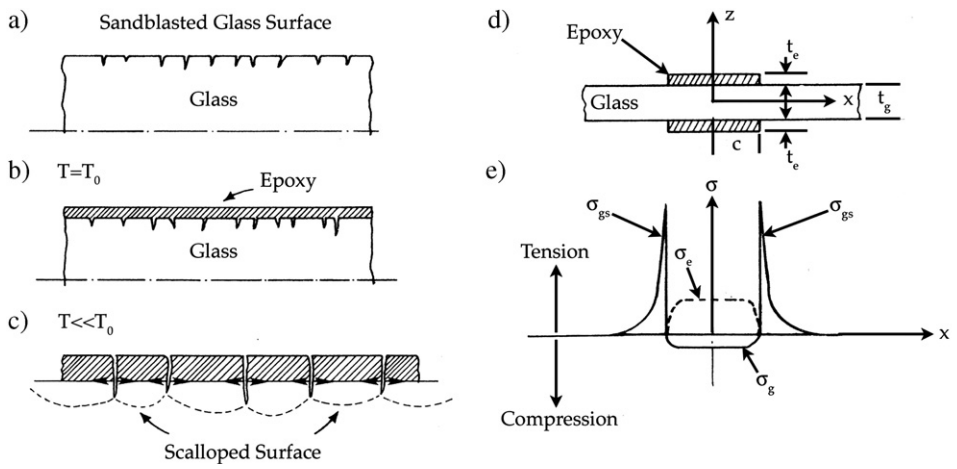

Fig. 9. (a–c) Schematic representation of the glue spall mechanism. (a) Sandblasted glass surface, (b) epoxy/glass composite at initial temperature, T_0, and (c) interface of composite, illustrating the islands of epoxy and the thin scallops of glass removed when $T \ll T_0$. (d–e) Schematic representation of an epoxy/glass/epoxy sandwich seal and the stress that arises in the composite. (d) Sandwich seal, dimensions and orientation. (e) Schematic of stress that arises in the glass surface under the epoxy, σ_g, in the epoxy, σ_e, and the glue spall stress around the boundary of the epoxy, σ_{gs}.

because hydrodynamic relaxation quickly dissipates this pressure as it arises. [The hydrodynamic relaxation time and diffusion coefficient used in these calculations are only valid at T=25–29 °C. However, the Stokes–Einstein equation indicates that the diffusion coefficient is inversely proportional to the fluid viscosity [76], so the ratio of the times is valid at any temperature.]

Osmotic pressure cannot account for the pessimum concentration because this pressure is maximized when internal crystallization occurs at very low temperature (about −15 °C) in a low concentration salt solution. In addition, osmotic pressure does not account for the absence of damage when the pool of solution is missing from the concrete surface.

3.4. Summary

Several mechanisms have been proposed that focus on the role of salts. None of these mechanisms adequately account for all of the characteristics of salt scaling. Field measurements indicate that the thermal shock realized when salt is applied to an ice layer on a concrete surface is not large enough to result in destructive stresses. Salt precipitation is not expected in the temperature range of scaling experiments; but even if it were, this mechanism would not account for the fact that organic solutes (ethanol and urea) produce results similar to those obtained with inorganic salts. It has been argued that the presence of salt in the pore solution increases the degree of saturation in the surface, which results in damage when the critical degree of saturation is surpassed. However, moderate salt concentrations, like those that result in the most severe scaling, do not result in a drastic increase in the degree of saturation. Lastly, this system will never experience destructive osmotic pressures. The osmotic pressure is limited by hydrodynamic relaxation, which has a characteristic time that is two orders of magnitude smaller than that necessary for the osmotic pressure to realize its potential.

4. Glue spalling

Recently, the glue spall mechanism was proposed as the primary cause of salt scaling [75,77]. Glue spalling is a technique used to decorate the surface of glass with uniform shallow scallops [78,79]. The procedure consists of sandblasting a glass surface, spreading a layer of epoxy over the surface at high temperature, and reducing the temperature of the composite (Fig. 9). As the temperature is reduced the epoxy tends to contract much more than the underlying glass, which places this layer in tension. Eventually, the epoxy fractures into many small islands. Along the perimeter of these islands a tensile stress forms in the glass (Fig. 9 — σ_{gs}). This glue spall stress causes flaws in the glass surface to propagate, culminating in the removal of a thin glass scallop. When a solution freezes on a concrete surface an ice/concrete bi-material composite forms. As the composite temperature is reduced below the melting point of the solution, the ice layer tends to contract 5 times as much as the underlying concrete [80–83]. Therefore, ice plays a role similar to the epoxy on a concrete surface [75,77].

Depending on the original solution concentration, the corresponding ice layer will crack under the tension imposed by the rigid concrete substrate [75,77]. Fracture mechanics allows us to predict how these cracks will behave [84–88]. It was previously shown [75,77] that cracks in the ice layer are expected to penetrate the underlying cementitious binder, and subsequently propagate into a path that is parallel to the composite interface, which results in the removal of a scallop. Therefore, with knowledge of the mechanical properties of the constituent materials, fracture mechanics allows us to account for both the occurrence and the morphology of damage due to the glue spall stress.

Here we systematically consider how the glue spall mechanism accounts for the characteristics listed in Section 1.

1. *Salt scaling consists of the progressive removal of small flakes or chips of binder.*

Fracture mechanics allows us to predict whether or not cracks in the ice layer will penetrate the concrete surface [85], and how they will behave when they do [86–88]. These analyses indicate that crack penetration, and the depth at which the crack turns parallel to the composite interface is dictated by the mechanical properties of the constituent materials. Therefore, if the properties of the concrete do not vary significantly in the surface, each freezing cycle will result in a relatively constant amount of damage. The damage morphology was accounted for in the previous paragraph.

2. *A pessimum exists at a solute concentration of ~3%, independent of the solute used.*
   The pessimum is a result of the effect of brine pockets (Fig. 6) on the mechanical properties of the ice layer. It was previously shown [75,77] that during a scaling experiment pure water ice is not expected to crack, brine ice formed from solutions of moderate concentration will crack, and highly concentrated solutions do not gain strength in the temperature range of interest. Therefore, only moderately concentrated brines result in scaling. Various solutes produce similar trends because they exhibit similar relationships between melting point depression and solute concentration (i.e., the shape of the liquidus, Fig. 6).
3. *No scaling occurs when the pool of solution is missing from the concrete surface.*
   There is no composite without the pool.
4. *No damage occurs when the minimum temperature is held above −10 °C;*
   Ice formed from a 3% NaCl solution, which is used in all conventional tests, does not have strength above this temperature [89].
   The amount of damage increases as the minimum temperature decreases below −10 °C.
   The glue spall stress is proportional to the undercooling, ΔT, so smaller and smaller flaws will propagate as the temperature drops.
5. *Air entrainment improves salt scaling resistance.*
   Air entrainment reduces bleeding [90,91], so it produces a stronger surface. Furthermore, when an effective air-entraining agent is properly utilized, initial freezing in air voids imposes suction in the pore fluid that compresses the porous skeleton (see Section 2.1). In fact, calculations similar to those presented in Section 2.1 indicate that compression of the porous matrix due to freezing in the air voids can reduce the damaging stresses due to the thermal expansion mismatch by one third (assuming $\rho=0.8$ for concrete or mortar). Therefore, cooling an air-entrained sample to −18 °C is equivalent to cooling a non-air-entrained sample no lower than −12 °C.
6. *The salt concentration of the pool on the surface is more important than the salt concentration in the pore solution.*
   The pore liquid has no effect on the severity of the glue spall stress, because internal ice formation does not play a role in salt scaling (see Section 2).
7. *Susceptibility to salt scaling is not correlated with susceptibility to internal frost action.*
   The glue spall mechanism is not related to internal crystallization.
8. *The strength of the surface governs the ability of a cementitious body to resist salt scaling.*
   The strength of the finished surface is important, because the estimated glue spall stress is marginal with respect to the tensile strength of the cementitious binder (~3 MPa). Any treatment or handling expected to weaken the surface (e.g., bleeding) will therefore result in more scaling. In fact, Marchand et al. indirectly verified the importance of surface strength by comparing results from finished and sawn surfaces. The authors showed that the amount of scaling was proportional to the amount of the surface covered by cementitious binder [92], which indicates that the much tougher aggregate prevents crack penetration.

5. Conclusions

In Part I of this series a comprehensive review of the experimental studies on salt scaling was presented, and the characteristics of this damage were summarized [11]. In this article, previously proposed mechanisms (including internal frost action) were considered. The feasibility of these mechanisms, as well as the characteristics of salt scaling, was used as a basis for judging adequacy. None of the previously proposed mechanisms is both feasible and capable of accounting for all characteristics of scaling damage. The glue spall mechanism was recently proposed as the cause of salt scaling, and we conclude that this mechanism adequately accounts for all the characteristics of this damage.

Acknowledgement

This work was supported by National Science Foundation Grant CMS-0200440.

References

[1] "Nonconventional Concrete Technologies: Renewal of the Highway Infrastructure", National Research Council, NMAB-484 (National Academy Press, Washington, DC, 1997).
[2] H. Arnfelt, Damage on Concrete Pavements by Wintertime Salt Treatment, Meddelande, vol. 66, Statens Väginstitut, Stockholm, 1943.
[3] G.J. Verbeck, P. Klieger, Studies of "salt" scaling of concrete, Highw. Res. Board. Bull. 150 (1957) 1–17.
[4] D. Jana, Concrete construction or salt — which causes scaling? Concr. Int. (Nov. 2004) 31–38.
[5] C. Alonso, C. Andrade, M. Castellote, P. Castro, Chloride threshold values to depassivate reinforcing bars embedded in a standardized OPC mortar, Cem. Concr. Res. 30 (2000) 1047–1055.
[6] W.G. Hime, The corrosion of steel — random thoughts and wishful thinking, Concr. Int. (Oct. 1993) 54–57.
[7] D. Beckett, Influence of carbonation and chlorides on concrete durability, Concrete (Feb. 1983) 16–18.
[8] G. Fagerlund, The international cooperative test of the critical degree of saturation method of assessing the freeze/thaw resistance of concrete, Mater. Constr. 10 (58) (1977) 230–251.
[9] G.W. Scherer, Crystalization in pores, Cem. Concr. Res. 29 (1999) 1347–1358.
[10] G.W. Scherer, J.J. Valenza, Mechanisms of frost damage, in: J. Skalny, F. Young (Eds.), Materials Science of Concrete, vol. VII, American Ceramic Society, 2005, pp. 209–246.

[11] J.J. Valenza II, G.W. Scherer, A review of salt scaling: I. Phenomenology, Cem. Concr. Res. (in press), doi:10.1016/j.cemconres.2007.03.005.
[12] T.C. Powers, A working hypothesis for further studies of frost resistance of concrete, J. Am. Concr. Inst. 16 (4) (1945) 245–272.
[13] T.C. Powers, Void spacing as a basis for producing air-entrained concrete, J. Am. Concr. Inst. 50 (1954) 741–760.
[14] T.C. Powers, The air-requirement of frost resistant concrete, Proc. Highway Res. Board, vol. 29, 1949, pp. 184–211.
[15] T.C. Powers, R.A. Helmuth, Theory of volume changes in hardened portland-cement paste during freezing, Proc. Highway Res. Board 32 (1953).
[16] S.J. Gregg, K.S.W. Sing, Adsorption, Surface Area and Porosity, 2nd ed. Academic, London, 1982.
[17] M. Brun, A. Lallemand, J.F. Quinson, C. Eyraud, A new method for the simultaneous determination of the size and the shape of pores: the thermoporometry, Thermochim. Acta 21 (1977) 59–88.
[18] G.G. Litvan, Phase transitions of adsorbates: III. Heat effects and dimensional changes in nonequilibrium temperature cycles, J. Colloid Interface Sci. 38 (1) (1972) 75–83.
[19] M.A. Biot, Theory of propagation of elastic waves in a fluid-saturated porous solid. I. Low frequency range, J. Acoust. Soc. Am. 28 (2) (1956) 168–178.
[20] M.A. Biot, General theory of three-dimensional consolidation, J. Appl. Phys. 12 (1941) 155–164.
[21] M.A. Biot, General solutions of the equations of elasticity and consolidation for a porous material, J. Appl. Mech. (Mar. 1956) 91–96.
[22] M.A. Biot, D.G. Willis, The elastic coefficients of the theory of consolidation, J. Appl. Mech. (Dec. 1957) 594–601.
[23] D.L. Johnson, Elastodynamics of gels, J. Chem. Phys. 77 (3) (1982) 1531–1539.
[24] O. Coussy, Mechanics of Porous Continua, Wiley, New York, 1995.
[25] G.W. Scherer, Measuring permeability of rigid materials by a beam-bending method: I. Theory, J. Am. Ceram. Soc. 83 (9) (2000) 2231–2239.
[26] W. Vichit-Vadakan, G.W. Scherer. Measuring permeability of rigid materials by the beam-bending method: II. Porous Vycor. J. Am. Ceram. Soc., 83 (9) (2000) 2240–2245.
[27] D.J. Corr, P.J. Monteiro, J. Bastacky, Microscopic characterization of ice morphology in entrained air voids, ACI Mater. J. 99-M18 (March-April 2002) 190–195.
[28] W. Vichit-Vadakan, G.W. Scherer. Measuring permeability of rigid materials by the beam-bending method: III. Cement Paste. J. Am. Ceram. Soc., 85 (6) (2002) 1537–544.
[29] J.P. Ciardullo, D.J. Sweeney, G.W. Scherer, Thermal expansion kinetics: method to measure the permeability of cementitious materials: IV. Effect of thermal gradients, J. Am. Ceram. Soc. 88 (5) (2005) 1213–1221.
[30] G. Fagerlund, The international cooperative test of the critical degree of saturation method of assessing the freeze/thaw resistance of concrete, Mater. Constr. 10 (58) (1977) 230–251.
[31] G. Fagerlund, The required air content of concrete, Contribution to the Workshop on “Mass Energy Transfer and Deterioration of Building Components”, Paris, January 1995.
[32] G. Fagerlund, Predicting the service life of concrete exposed to frost action through modelling of the water absorption process in the air-pore system, Lund Institute of Technology, Div. of Building Materials, Report TVBM-7085, 1994.
[33] G. Fagerlund, Moisture uptake and service life of concrete exposed to frost, in: K. Sakai, N. Banthia, O.E. Gjørv (Eds.), Proceedings of the International Conference on Concrete under Severe Conditions, Sapporo, Japan, vol. 1, E & FN Spon, Tokyo, Aug. 2–4 1995.
[34] W.B. Hillig, D. Turnbull, Theory of crystal growth in undercooled pure liquids, J. Chem. Phys. 24 (1956) 914.
[35] G.W. Scherer, Freezing gels, J. Non-Cryst. Solids 155 (1993) 1–25.
[36] T.C. Powers, Freezing effects in concrete, Durability of Concrete, ACI SP-47, 1975, pp. 1–11.
[37] R.A. Helmuth, Discussion of the paper ‘Frost action in concrete’ by P. Nerenst; pp. 829–833 in Proceedings of the 4th International Congress on Chemistry of Cement, vol. 2. NBS Monograph 43. National Bureau of Standards, Washington DC, 1962.
[38] J.J. Beaudoin, C. MacInnis, The mechanism of frost damage in hardened cement paste, Cem. Concr. Res. 4 (2) (1974) 139–147.
[39] F.P. Browne, P.D. Cady, Deicer scaling mechanisms in concrete, Am. Concr. Inst. SP-47 (1975) 101–119.
[40] A.E. Corte, Vertical migration of particles in front of a moving freezing plane, J. Geophys. Res. 67 (3) (1962) 1085–1090.
[41] D.R. Uhlmann, B. Chalmers, Interaction between particles and a solid–liquid interface, J. Appl. Phys. 35 (10) (1964) 2986–2993.
[42] A.A. Chernov, D.E. Temkin, A.M. Mel’nikova, Theory of the capture of solid inclusions during the growth of crystals from the melt, Sov. Phys. Cryst. 21 (4) (Jul.-Aug. 1976) 369–373.
[43] K.A. Jackson, D.R. Uhlmann, B. Chalmers, Frost heave in soils, J. Appl. Phys. 37 (2) (1966) 848–852.
[44] K.A. Jackson, B. Chalmers, Freezing of liquids in porous media with special reference to frost heave in soils, J. Appl. Phys. 29 (8) (1958) 1178–1181.
[45] S. Taber, Frost heaving, J. Geol. 37 (1929) 428–461.
[46] S. Taber, The mechanics of frost heaving, J. Geol. 38 (1930) 303–317.
[47] S. Taber, Freezing and thawing in soils as factors in the destruction of road pavements, Public Roads 11 (6) (1930) 113–132.
[48] S. Lowell, J.E. Shields, Powder surface Area and Porosity, Chapman and Hall, New York, 1984.
[49] S. Mindness, J.F. Young, Concrete, Prentice-Hall, Inc., Englewood Cliffs, NJ, 1981, p. 212.
[50] A.M. Neville, Properties of Concrete, John Wiley and Sons, Inc., New York, NY, 1996.
[51] D.H. Everett, The thermodynamics of frost damage to porous solids, Trans. Faraday Soc. 57 (1961) 1541–1551.
[52] O. Coussy, Poromechanics of freezing materials, J. Mech. Phys. Solids 53 (2005) 1689–1718.
[53] G.W. Scherer, J. Chen, and J. Valenza, Method of protecting concrete from freeze/damage, U.S. Patent 6 485 560 (Nov. 26, 2002).
[54] S. Chatterji, Freezing of air-entrained cement-based materials and specific actions of air-entraining agents, Cem. Concr. Res. 25 (2003) 759–765.
[55] R.C. Mielenz, V.E. Volkodoff, J.E. Backstrom, H.L. Flack, Origin, evolution, and effects of the air void system in concrete: Part I. Entrained air in unhardened concrete, ACI Mater. J. 55 (1958) 95–121.
[56] G. Fagerlund, Studies of the destruction mechanisms at freezing of porous materials, Contributions to Fondation Française d’Études Nordiques, Vie Congres Int. Les problèmes poses par la gélifraction. Recherches fondamentales et appliqués, (French Foundation for Nordic Studies, 6th International congress on Problems Raised by Freezing. Fundamental and Applied Research), Le Havre, 23–25 April 1975.
[57] J. Marchand, M. Pigeon, D. Bager, C. Talbot, Influence of chloride solution concentration of salt scaling deterioration of concrete, ACI Mater. J. (July-Aug 1999) 429–435.
[58] E.J. Sellevold, T. Farstad, Frost/Salt testing of concrete: effect of test parameters and concrete moisture history, Nord. Concr. Res. 10 (1991) 121–138.
[59] R.E. Beddoe, M.J. Setzer, A low temperature DSC investigation of hardened cement paste subjected to chloride action, Cem. Concr. Res. 18 (1988) 249–256.
[60] F.T. Wall, Chemical Thermodynamics, Freeman, San Francisco, 1965.
[61] A. Rösli, A.B. Harnik, Improving the durability of concrete to freezing and deicing salts, in: P.J. Sereda, G.G. Litvan (Eds.), Durability Build. Mater. and Components. ASTM Special Technical Publication STP-691, ASTM, Philadelphia, 1980, pp. 464–473.
[62] T. Ye, Z. Suo, T. Evans, Thin film cracking and the roles of substrate and interface, Int. J. Solid Struct. 29 (21) (1992) 2639–2648.
[63] J. Weissenberger, G. Dieckmann, R. Gradinger, M. Spindler, Sea ice: a cast technique to examine and analyze brine pockets and channel structure, Limnol. Oceanogr. 37 (1) (1992) 179–183.
[64] D.A. Porter, K.E. Easterling, Phase Transformations in Metals and Alloys, 2nd Ed. Stanley Thornes, Cheltenham, UK, 1992.
[65] L. Binda, G. Baronio, Mechanism of masonry decay due to salt crystallization, Durability Build. Mater. 4 (1987) 227–240.
[66] Q. Yang, X. Wu, S. Huang, Concrete deterioration due to physical attack by salt crystallization, Proc. 10th International Congress on the Chemistry of Cement, Gothenburg, 1997, paper 4iv032.
[67] R.C. Weast, M.J. Astle (Eds.), CRC Handbook of Chemistry and Physics, 62nd ed., CRC Press, Boca Raton, FL, 1981.

[68] G.W. Scherer, Stress from crystallization of salt, Cem. Concr. Res. 34 (2004) 1613–1624.
[69] B. Lubelli, R.P.J. van Hees, H.P. Huinink, C.J.W.P. Groot, Irreversible dilation of NaCl contaminated lime-cement mortar due to crystallization cycles, Cem. Concr. Res. 36 (2006) 678–687.
[70] J. Marchand, B. Gerard, and A. Delgrave, Ion Transport Mechanisms in Cement-Based Materials, pp. 307–399 in *Materials Science of Concrete??*, eds. J. Skalny and S. Mindess (Am. Ceram. Soc., Westerville, OH, ??).
[71] K. Denbigh, The Principles of Chemical Equilibrium, 2nd Ed.Cambridge Univ. Press, 1966.
[72] G.G. Litvan, Phase transition of adsorbates: Part VI. Effect of deicing agents on the freezing of cement paste, J. Am. Ceram. Soc. 58 (1–2) (1975) 26–30.
[73] C. MacInnis, J.D. Whiting, The frost resistance of concrete subject to a deicing agent, Cem. Concr. Res. 9 (1979) 325–336.
[74] J.J. Valenza, G.W. Scherer, Measuring the permeability of rigid materials by a beam-bending method: V. Isotropic rectangular plates of cement paste, J. Am. Ceram. Soc. 87 (10) (2004) 1927–1931.
[75] J.J. Valenza II, Mechanism for salt scaling, PhD thesis, Princeton University (2005). www.jvalenza.com/thesis.html.
[76] R.B. Bird, W.E. Stewart, E.N. Lightfoot, Transport Phenomena, Wiley, New York, 1960.
[77] J.J. Valenza, G.W. Scherer, Mechanism for salt scaling, J. Am. Ceram. Soc. 89 (4) (2006) 1161–1179.
[78] S.T. Gulati, H.E. Hagy, Analysis and measurement of glue-spall stresses in glass-epoxy bonds, J. Am. Ceram. Soc. 65 (1) (1982) 1–5.
[79] S.T. Gulati, H.E. Hagy, Theory of the narrow sandwich seal, J. Am. Ceram. Soc. 61 (5–6) (1973) 260–263.
[80] G.W. Scherer, Characterization of saturated porous bodies, Concr. Sci. Eng. 37 (265) (2004) 21–30.
[81] J.P. Ciardullo, D.J. Sweeney, G.W. Scherer, Thermal expansion kinetics: method to measure the permeability of cementitious materials: IV. Effect of thermal gradients, J. Am. Ceram. Soc. 88 (5) (2005) 1213–1221.
[82] E.R. Pounder, Physics of Ice, Pergamon Press, Oxford, 1965.
[83] R.E. Gagnon, S.J. Jones, Elastic properties of ice, in: M. Levy, H. Bass, R. Stern (Eds.), Elastic Properties of Solids: Biological and Organic Materials (Chapter 9), Handbook of Elastic Properties of Solids, Liquids, and Gases, vol. III, Academic Press, New York, 2001, pp. 229–257.
[84] L.E. Raray, D. Tabor, The adhesion and strength properties of ice, Proc. R. Soc. Lond., A 245 (1241) (1958) 184–201.
[85] T. Ye, Z. Suo, T. Evans, Thin film cracking and the roles of substrate and interface, Int. J. Solid Struct. 29 (1992) 2639–2648.
[86] M.D. Thouless, A.G. Evans, M.F. Ashby, J.W. Hutchinson, The edge cracking and spalling of brittle plates, Acta Metall. 35 (6) (1987) 1333–1341.
[87] M.D. Drory, M.D. Thouless, A.G. Evans, On the decohesion of residually stressed thin films, Acta Metall. 36 (8) (1998) 2019–2028.
[88] M.D. Drory, A.G. Evans, Experimental observations of substrate fracture caused by residually stressed films, J. Am. Ceram. Soc. 73 (3) (1990) 634–638.
[89] W.F. Weeks, Tensile strength of NaCl ice, J. Glaciol. 4 (1962) 25–52.
[90] G.M. Bruere, Mechanisms by which air-entraining agents affect viscositites and bleeding properties of cement pastes, Aust. J. Appl. Sci. 9 (1958) 349–359.
[91] T.C. Powers, The Properties of Fresh Concrete, John Wiley and Sons, Inc., New York, 1968.
[92] J. Marchand, M. Pigeon, J. Boisvert, H.L. Isabelle, O. Houdusse, Deicer salt scaling resistance of roller compacted concrete pavements containing fly ash and silica fume, in: V.M. Malhotra (Ed.), ACI Special Publication SP-132, 1992, pp. 151–178.